RdgB2 is required for dim-light input into intrinsically photosensitive retinal ganglion cells

Marquis T. Walker[a], Alan Rupp[b], Rebecca Elsaesser[a], Ali D. Güler[b,c], Wenlong Sheng[d], Shijun Weng[d,e], David M. Berson[e], Samer Hattar[b], and Craig Montell[a,f]

[a]Department of Biological Chemistry, Johns Hopkins University School of Medicine, Baltimore, MD 21205; [b]Department of Biology, Johns Hopkins University, Baltimore, MD 21218; [c]Department of Biology, University of Virginia, Charlottesville, VA 22903; [d]Institute of Neurobiology, Institute of Brain Science and State Key Laboratory of Medical Neurobiology, Fudan University, Shanghai 200032, China; [e]Department of Neuroscience, Brown University, Providence, RI 02912; [f]Neuroscience Research Institute and Department of Molecular, Cellular and Developmental Biology, University of California, Santa Barbara, Santa Barbara CA 93106

ABSTRACT A subset of retinal ganglion cells is intrinsically photosensitive (ipRGCs) and contributes directly to the pupillary light reflex and circadian photoentrainment under bright-light conditions. ipRGCs are also indirectly activated by light through cellular circuits initiated in rods and cones. A mammalian homologue (RdgB2) of a phosphoinositide transfer/exchange protein that functions in *Drosophila* phototransduction is expressed in the retinal ganglion cell layer. This raised the possibility that RdgB2 might function in the intrinsic light response in ipRGCs, which depends on a cascade reminiscent of *Drosophila* phototransduction. Here we found that under high light intensities, *RdgB2*^{−/−} mutant mice showed normal pupillary light responses and circadian photoentrainment. Consistent with this behavioral phenotype, the intrinsic light responses of ipRGCs in *RdgB2*^{−/−} were indistinguishable from wild-type. In contrast, under low-light conditions, *RdgB2*^{−/−} mutants displayed defects in both circadian photoentrainment and the pupillary light response. The RdgB2 protein was not expressed in ipRGCs but was in GABAergic amacrine cells, which provided inhibitory feedback onto bipolar cells. We propose that RdgB2 is required in a cellular circuit that transduces light input from rods to bipolar cells that are coupled to GABAergic amacrine cells and ultimately to ipRGCs, thereby enabling ipRGCs to respond to dim light.

INTRODUCTION

The mammalian retina comprises three broad types of photoreceptor cells that capture light and initiate visual signaling (Hattar *et al.*, 2003; Berson, 2007). Two classes of photoreceptor cells—rods and cones—are located in the outer retina, and their function is essential for image formation. In addition, ~1–2% of the retinal ganglion cells (RGCs) in the inner retina are intrinsically photosensitive (ipRGCs; Hattar *et al.*, 2002, 2006; Berson, 2007) and contribute to non–image-forming functions—circadian photoentrainment and the pupillary light reflex (Berson, 2007).

The ipRGCs respond directly to bright (photopic) light through a signaling cascade that is remarkably similar to that used in *Drosophila* photoreceptor cells. Light activation is initiated by the photopigment melanopsin, which is biophysically and molecularly related to fly rhodopsins (Terakita, 2005; Nickle and Robinson, 2007). Melanopsin engages a heterotrimeric G-protein that couples to phospholipase C (PLC) and TRPC channels similar to those used in *Drosophila* phototransduction (Isoldi *et al.*, 2005; Qiu *et al.*, 2005; Xue *et al.*, 2011).

In addition to sensing light directly, ipRGCs are also activated indirectly by light captured by rods and cones (Lucas *et al.*, 2003; Mrosovsky and Hattar, 2003; Wong *et al.*, 2007; Altimus *et al.*, 2008; Güler *et al.*, 2008; Weng *et al.*, 2013). Indirect, rod-mediated activation allows ipRGCs to respond to very dim (scotopic) stimuli that are

subthreshold for the direct melanopsin/Gq/PLC/TRPC-mediated photoresponse. Because ipRGCs are essentially the sole source of retinal input to the circadian and pupillary systems, rod influences on the ipRGCs permit animals to entrain their circadian rhythms and constrict their pupils in response to light stimuli in the scotopic range.

The indirect mode for ipRGC activation is not well understood. No signaling protein has been identified that affects this pathway, and multiple cellular circuits have been proposed to couple light activation of rods to stimulation of ipRGCs (Lucas *et al.*, 2003; Mrosovsky and Hattar, 2003; Østergaard *et al.*, 2007; Wong *et al.*, 2007; Altimus *et al.*, 2008; Güler *et al.*, 2008; Weng *et al.*, 2013). It has been proposed that the main circuit couples rods to rod bipolar cells, amacrine cells, and cone bipolar cells, which ultimately stimulate ipRGCs. Amacrine cells are synaptically active in the inner plexiform layer (IPL) and function in signal integration, modulation, and temporal filtering (Kolb, 1995, 1997) These cells modulate visual signals received by RGCs through lateral inhibitory feedback on bipolar cells. GABAergic amacrine cells provide inhibitory feedback to rod and cone bipolar cells through the release of the neurotransmitter γ-aminobutyric acid (GABA). Bipolar cells also receive GABAergic input from horizontal cells in the outer plexiform layer, but the major inhibitory input comes from amacrine cells in the IPL (Euler and Wässle, 1998), which help to maintain response sensitivity in the bipolar cells (Chávez *et al.*, 2006, 2010; Schubert *et al.*, 2013).

Here we report that the mouse homologue of *Drosophila* Retinal Degeneration B (RDGB), referred to as RdgB2, affects the rod-driven light input into ipRGCs. The fly and mouse proteins share 46% amino acid identity and include an N-terminal ~280–amino acid region that is similar to phosphatidylinositol transfer proteins (Lu *et al.*, 1999). Fly RDGB is expressed in photoreceptor cells, and loss of this protein impairs termination of phototransduction (Harris and Stark, 1977; Milligan *et al.*, 1997). Mouse RDGB is expressed in the inner retina, and *RdgB2⁻/⁻* mutant animals are reported to display a visual response indistinguishable from that of wild-type animals (Lu *et al.*, 2001). However, this analysis predated the discovery of the ipRGCs.

In the present work, we reinvestigated a potential role of RdgB2 during light processing by ipRGCs. We found that mutation of *RdgB2* did not disrupt melanopsin-dependent phototransduction. Instead, RdgB2 was expressed in a subset of GABAergic amacrine cells, and these cells depended on RdgB2 to maintain rod input to ipRGCs. Loss of RdgB2 reduced the pupillary light response and circadian photoentrainment but only under scotopic conditions. These results demonstrate the need for RdgB2 to maintain dim-light sensitivity in ipRGCs. Thus RdgB2-expressing cells function at the intersection of image-forming and non–image-forming pathways and promote the rod input that contributes to non–image-forming behavior in dim light.

RESULTS
Retinal expression of RdgB2
The RdgB2 protein is expressed in the inner layers of the retina (Lu *et al.*, 1999, 2001). To characterize the spatial distribution in greater detail, we performed immunostaining using RdgB2 antibodies. Consistent with a previous report (Lu *et al.*, 2001), anti-RdgB2 stained cells in the inner nuclear layer (INL) and the ganglion cell layer (GCL) of wild-type but not *RdgB2⁻/⁻* retina (Figure 1, A–C). The GCL contains RGCs and displaced amacrine cells (Schmidt *et al.*, 1985; Perez De Sevilla Müller *et al.*, 2007), whereas the INL is composed of three types of interneurons: bipolar, horizontal, and amacrine cells. Both bipolar and amacrine cells synapse onto ganglion cells and transmit light responses from rod and cone photoreceptor cells (Kolb, 1997; Chávez *et al.*, 2006; Dumitrescu *et al.*, 2009; Masland, 2011; Asari and Meister, 2012). In the INL, RdgB2 immunostaining appeared to be restricted to amacrine cells, since the staining was exclusively in the proximal region of the INL directly adjacent to the IPL (Figure 1, A and B), and bipolar and horizontal cells are found only more distally in the INL. Moreover, there was no costaining between anti-RdgB2 and the rod bipolar cell marker anti–protein kinase Cα (PKCα; Figure 1, D–F). Thus RdgB2 was expressed in amacrine cells and cells in the GCL. The overall thickness of the GCL, the INL, and the outer nuclear layer (ONL; Figure 1, B and C) of the *RdgB2⁻/⁻* retina was not distinguishable from wild-type, indicating that there was no significant degeneration, consistent with a previous report (Lu *et al.*, 2001).

RdgB2 functions in pupillary constriction under low light
Based on the localization of RdgB2 in the GCL and the amino acid sequence homology of mammalian RdgB2 with *Drosophila* RDGB, which functions in fly photoreceptor cells, we considered that RdgB2 might contribute to the invertebrate-like phototransduction pathway in ipRGCs. To test for a possible requirement for RdgB2 in the melanopsin-dependent photoresponse, we measured the pupillary light reflex (PLR; Figure 2A). As shown previously, loss of melanopsin (OPN4) impaired the PLR using phototopic light (Figure 2B; Hattar *et al.*, 2003; Lucas *et al.*, 2003; Mrosovsky and Hattar, 2003). However, *RdgB2⁻/⁻* mice displayed a normal PLR (Figure 2B).
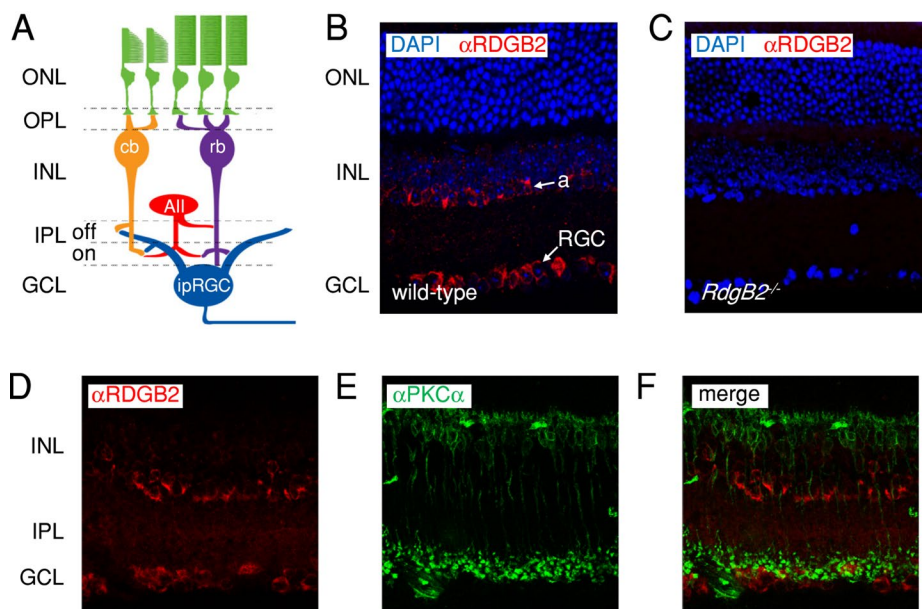
FIGURE 1: RdgB2 expression in the mouse retina. (A) Diagram of retinal layers. Outer nuclear layer (ONL), outer plexiform layer (OPL), inner nuclear layer (INL), inner plexiform layer (IPL), synaptic layers where ON bipolar (on) or OFF bipolar (off) cell axons project, and ganglion cell layer (GCL). Labeled neurons: AII amacrine (AII), ON cone bipolar cells (cb), M1 ipRGCs (ipRGC), and rod bipolar cells (rb). (B, C) Immunofluorescence staining of wild-type and *RdgB2⁻/⁻* retinal slices with anti-RdgB2. Amacrine cell (a) and retinal ganglion cell (RGC). (D–F) immunofluorescence staining of a wild-type retinal slice with anti-RdgB2 and anti-PKCα.
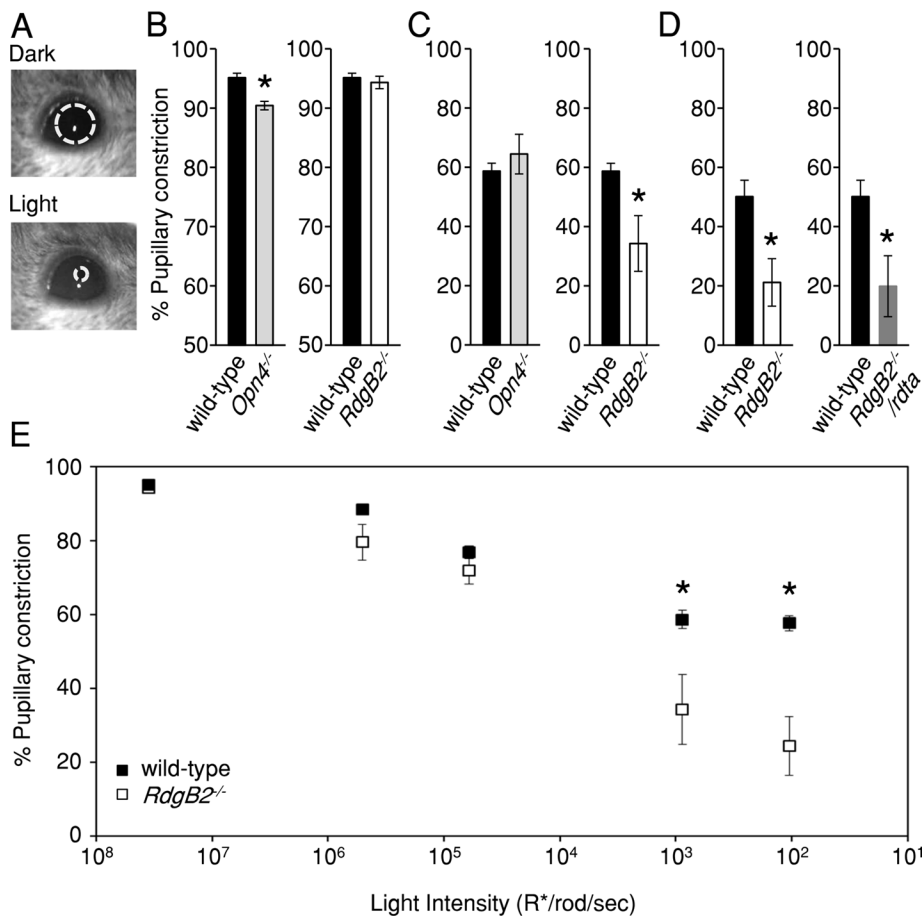
FIGURE 2: Pupillary light responses under phototopic and scotopic illumination. (A) Images of mouse eyes used to measure pupil area before and after light stimulation. wt, wild-type. (B) Pupillary constriction under bright blue light (3.51×10^7 R*/rod per second). The light intensities were controlled using neutral density (ND) filters. (C, D) Pupillary constriction under dim blue light (8.74×10^2 and 1.26×10^1 R*/rod per second, respectively). (E) Irradiance–response curve measuring pupillary constriction in response to decreasing intensities of blue light. Light intensities: 3.51×10^7, 5.06×10^5, 6.07×10^4, 8.74×10^2, and 1.05×10^2 R*/rod per second. Pupillary constriction = [1 − (light pupil area/dark pupil area)] × 100. $n = 4$–6. Error bars indicate ±SEM. Statistical significance was determined using unpaired Student's t tests (B–D) and one-way analysis of variance and Tukey post hoc test. *$p \leq 0.05$.

Pupil constriction occurs over a wide range of light intensities. Melanopsin is sufficient for constriction in bright light, but cone or rod input is required to drive constriction under dim light (Güler et al., 2008; Altimus et al., 2010; Weng et al., 2013). Indirect rod and cone input allows the ipRGCs to be activated under scotopic light conditions, which are insufficient to stimulate melanopsin (Altimus et al., 2008; Güler et al., 2008; Weng et al., 2013). We found that when we decreased the light intensity to scotopic levels, *RdgB2⁻/⁻* mice showed a pronounced decline in pupillary constriction (Figure 2, C and E), whereas the PLR of *Opn4⁻/⁻* mice was similar to that of wild-type (Figure 2C). As we decreased the light intensities, the difference between the wild-type and mutant animals became greater (Figure 2E).

Because wild-type and *RdgB2⁻/⁻* mice showed the same PLR under photopic conditions, our results suggested that RdgB2 was not required for melanopsin-driven responses in ipRGCs. Instead, loss of RdgB2 activity caused a decrease in response to scotopic light intensities and appeared to disrupt rod input into ipRGCs. If RDGB2 is essential for all rod input for the PLR, then blocking rod activity in combination with the *RdgB2⁻/⁻* mutation should result in an impair-

ment that is no more severe than that resulting from the *RdgB2⁻/⁻* mutation alone. To disrupt rod photoreceptors, we genetically ablated these cells by expressing tetanus toxin in rods (*rdta* transgene; Freedman et al., 1999). We found that the PLR in the *RdgB2⁻/⁻*; *rdta* animals under dim light matched that of the *RdgB2⁻/⁻* knockout alone (Figure 2D).

## Photoactivity of ipRGCs in *RdgB2⁻/⁻* mutant retinas

Although RdgB2 is expressed in the GCL, the PLR data suggest that RdgB2 does not function in melanopsin-dependent photo-transduction. In further support of this conclusion, we did not detect any overlap between anti-RdgB2 and anti-melanopsin staining (Figure 3, A–C). These findings indicate that RdgB2 affects ipRGC activity in a non–cell-autonomous way through external visual pathways that provide input into ipRGCs.

To test the conclusion that *RdgB2* does not function in ipRGCs, consistent with the immunostaining data, we used multielectrode arrays (MEAs) to compare the light responses in wild-type and *RdgB2⁻/⁻* retinas. MEAs provide the ability to record from multiple ipRGCs, which are sparsely distributed across the retina. We stimulated the retinas with whole-field flashes of increasing intensity in the presence of synaptic blockers and found no differences in the number or rate of light-driven action potentials elicited by the ipRGCs of *RdgB2⁻/⁻* and wild-type mice (Figure 3, D and E). Moreover, ipRGCs in *RdgB2⁻/⁻* animals exhibited the same characteristic long latency of activation and slow termination of the responses observed in wild-type ipRGCs (Figure 3, F and G). Thus the ipRGCs exhibited normal photoactivity in *RdgB2⁻/⁻* animals, further indicating that RdgB2 was not involved in melanopsin-initiated light responses.

RdgB2-expressing amacrine cells are GABAergic

Amacrine cells regulate bipolar cells and promote input into the ipRGCs through retinal circuits initiated in rods and cones (Wong et al., 2007; Dumitrescu et al., 2009; Altimus et al., 2010; Chávez et al., 2010; Demb and Singer, 2012; Weng et al., 2013). Morphologically, there are ~30 types of amacrine cells that are either GABAergic or glycinergic (Perez De Sevilla Müller et al., 2007; Masland, 2011). In addition, dopaminergic amacrine cells, which are also GABAergic, receive input from and are closely associated with ipRGCs (Zhang and McCall, 2012). In a reciprocal manner, ipRGCs receive input from all broad neurotransmitter types of amacrine cell—dopaminergic, glycinergic, and GABAergic (Perez De Sevilla Müller et al., 2007; Wong et al., 2007; Dumitrescu et al., 2009; Van Hook et al., 2012). Moreover, the melanopsin-driven light responses of ipRGCs are modulated by dopamine through D1 dopamine receptors (Van Hook et al., 2012).
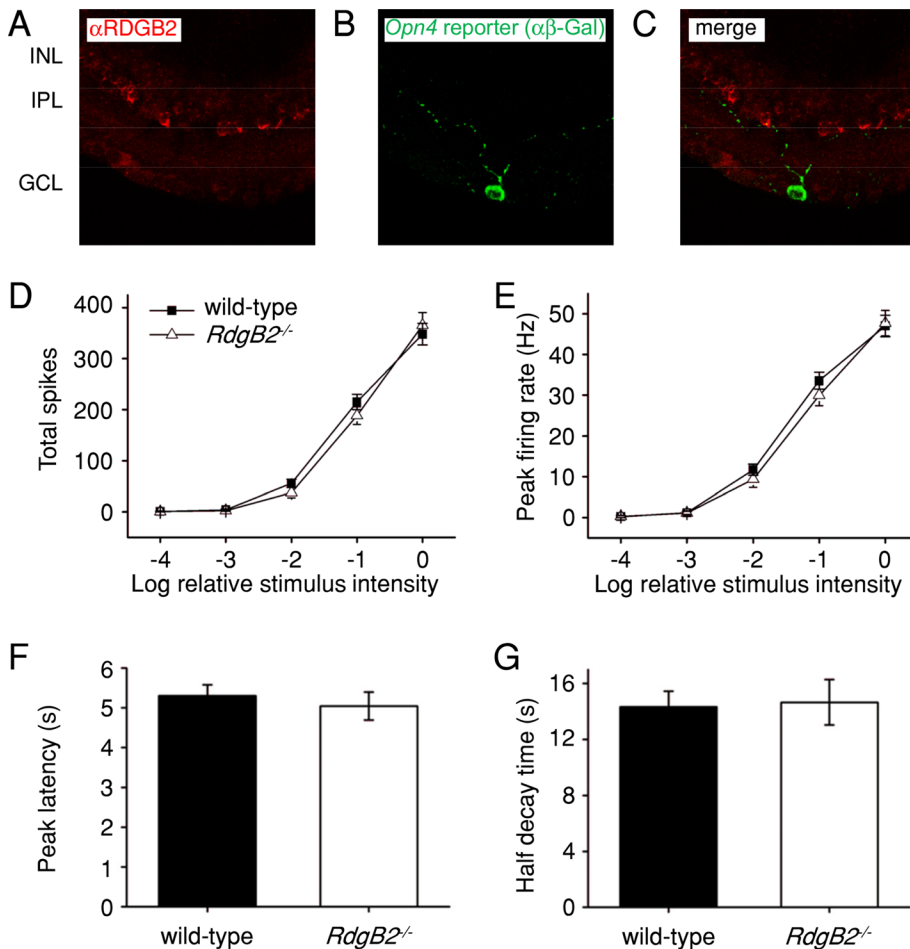
FIGURE 3: Relative responses of melanopsin-driven RGCs (ipRGCs) from wild-type and *RdgB2*⁻/⁻ mice using multielectrode array recordings. (A–C) immunofluorescence staining of a retinal slice from an *Opn4*⁻/⁻ mouse with a *tau-lacZ* transgene knocked into the *Opn4* locus with anti-RdgB2 and anti–β-Gal. (D, E) Intensity–response relationships at increasing light intensities. (D) Total spikes. (E) Peak firing rates. (F, G) Intrinsic light response measurements at 0 log intensity. (F) Peak latency. (G) Half decay time. The error bars represent ±SEM. Wild-type, *n* = 85; *RdgB2*⁻/⁻, *n* = 44. There were no statistically significant differences on the basis of unpaired Student's *t* tests.

To test whether RdgB2-positive amacrine cells were dopaminergic, we stained retinal slices with anti-RdgB2 and antibodies to tyrosine hydroxylase, an enzyme essential for the synthesis of dopamine. The RdgB2-positive amacrine cells greatly outnumbered the tyrosine hydroxylase (TH)–positive cells, and there was no colocalization (Figure 4, A–C). In contrast, 100% of the anti-RdgB2–positive cells costained with anti-GABA (Figure 4, D–F). These findings indicate that the amacrine cells that express RdgB2 are GABAergic.

RdgB2⁻/⁻ display an impairment in the b-wave of the electroretinogram, suggesting a requirement for GABA-driven inhibitory feedback

Electroretinogram (ERG) recordings measure light-evoked changes in activity across the retina and include a- and b-wave components. The downward deflection of the a-wave reflects light-induced closing of the channels in the photoreceptor cells (Figure 5, A and B). After light stimulation of rods and cones, the b-wave results from depolarization of cells downstream of the photoreceptor cells, especially bipolar cells (Figure 5, A and B). The amplitude of the b-wave is modulated by GABA-mediated lateral inhibition (Euler and Wässle, 1998; Eggers and Lukasiewicz, 2006; Smith *et al.*, 2013). Pharmacological blocking of GABA$_c$ receptors in the retina causes

decreased b-wave amplitude (Euler and Wässle, 1998; Eggers and Lukasiewicz, 2006; Smith *et al.*, 2013). Bipolar cells receive GABAergic input from horizontal cells in the outer plexiform layer, but the major portion of the inhibitory input comes from amacrine cells in the IPL (Figure 5A; Euler and Wässle, 1998). Owing to expression of RdgB2 in GABAergic amacrine cells, we examined the b-wave of the ERG.

We found that the *RdgB2*⁻/⁻ mouse ERGs displayed a decrease in b-wave amplitude relative to wild-type mice. At scotopic light intensities, *RdgB2*⁻/⁻ mice displayed ~15% decrease in the b-wave (Figure 5, B and C). Surprisingly, given the impairment in PLR only under scotopic conditions (Figure 2), the difference in b-wave amplitude was greatest under photopic conditions (~40%; Figure 5, D and E), which we established using a bright flash over background light that saturated the rods. The a-wave was indistinguishable between wild-type and *RdgB2*⁻/⁻ mutant animals.

Circadian entrainment impaired under scotopic conditions in *RdgB2*⁻/⁻ mice

In addition to the PLR, light signaling via ipRGCs is necessary for circadian photoentrainment (Freedman *et al.*, 1999; Altimus *et al.*, 2008). To test whether RdgB2 also promotes photoentrainment, we exposed wild-type and mutant animals to 12 h:12 h light/dark cycles. After 2 wk of entrainment, we advanced the onset of darkness by 6 h and gradually decreased the light intensities during the light period of the light/dark cycles. The light steps we used covered a broad range of intensities, starting with bright conditions and following by progressive reduc-

tions in light until the intensity was very dim. All of the animals entrained to the brightest light intensity (Figure 6A). As we decreased the light intensity, *RdgB2*⁻/⁻ mice were slower to phase shift their activity onset to the start of the dark period (Figure 6, A and B). When the ambient light was decreased to 1 lux, we observed a significant increase in the number of days required for *RdgB2*⁻/⁻ mice to entrain to the dim light intensity (Figure 6B). At the lowest light intensity (0.2 lux), the median time required by the *RdgB2*⁻/⁻ mice to reentrain was much slower than that for the wild-type animals (wild-type, 17 d; *RdgB2*⁻/⁻, 27 d), although the difference was not statistically significant due to the large variations (Figure 6B). Although *RdgB2*⁻/⁻ mice displayed impaired dim-light photoentrainment, they showed wild-type period lengths at all light intensities (Figure 6C). These results showed that under scotopic conditions, RdgB2 was required for normal photoentrainment.

DISCUSSION
The ipRGCs function primarily in promoting light-induced functions, such as the pupillary light reflex and photoentrainment of circadian rhythm (Freedman *et al.*, 1999; Gooley *et al.*, 2003; Hattar *et al.*, 2003; Lucas *et al.*, 2003; Mrosovsky and Hattar, 2003; Berson, 2007). These behaviors are elicited by bright light through direct activation of the
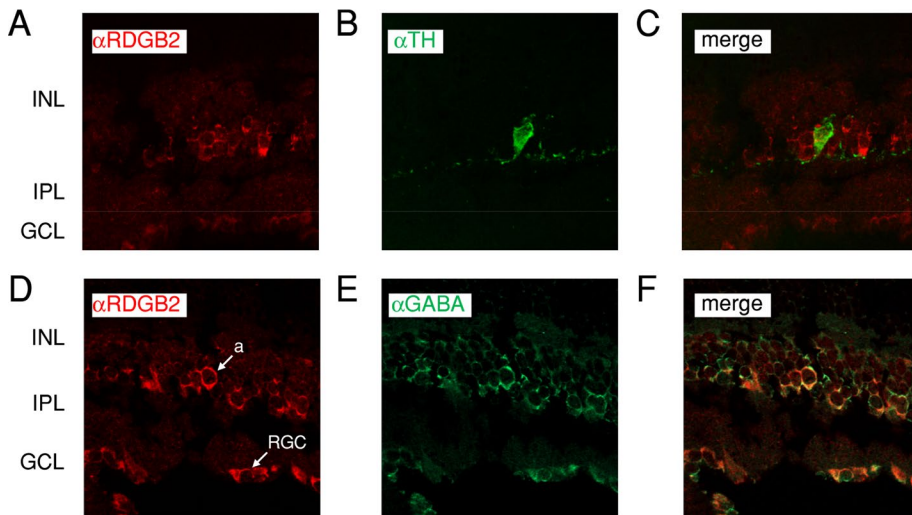
FIGURE 4: Immunofluorescence staining of the retina to detect neurotransmitter expression in RdgB2-positive cells. (A–C) immunofluorescence staining of a wild-type retinal slice with anti-RdgB2 and anti-TH. (D–F) immunofluorescence staining of a wild-type retinal slice with anti-RdgB2 and anti-GABA.

melanopsin-dependent phototransduction cascade in ipRGCs (Berson *et al.*, 2002; Lucas *et al.*, 2003; Wong *et al.*, 2005). In addition, dim light that is insufficient for initiating effective intrinsic phototransduction in ipRGCs can still drive these behaviors through input from outer retinal photoreceptors (Lucas *et al.*, 2003; Mrosovsky and Hattar, 2003; Wong *et al.*, 2007; Altimus *et al.*, 2008; Güler *et al.*, 2008; Weng *et al.*, 2013). The latter mechanism for stimulating ipRGCs begins with photoactivation of rods. However, the signaling molecules that participate in connecting the rod-driven pathway to ipRGCs were unknown.

Our study indicates that an indirect, rod-driven pathway for activating ipRGCs depends in part on RdgB2, the mouse homologue of *Drosophila* RDGB (Lu *et al.*, 1999), which functions in the fly visual response (Harris and Stark, 1977; Milligan *et al.*, 1997). In support of this conclusion, circadian photoentrainment and the PLR were impaired in *RdgB2*$^{-/-}$ mutant animals, but only under scotopic light conditions that were too low for effective activation of melanopsin.

Our findings lead us to conclude that RdgB2 functions in a cellular circuit postsynaptic to rods rather than in the rods themselves. RdgB2 was not expressed in rod photoreceptor cells but was in the inner retina. Thus, as previously reported (Lu *et al.*, 2001), RdgB2 does not appear to function in the outer retina. These results provide the first demonstration that RdgB2 has a functional role in light signaling in the mammalian retina, and the ERG results indicate that it functions downstream of the photoreceptors in the outer retina.

We found that RdgB2 is expressed in GABA-positive amacrine cells, as well as in a subset of cells in the GCL. However, RdgB2 does not appear to function in the light response in ipRGCs, since the MEA recordings were similar in wild-type and *RdgB2*$^{-/-}$ retinas, consistent with normal circadian entrainment and PLR under phototopic light. Moreover, RdgB2 was not colocalized with melanopsin, which is expressed and required in ipRGCs.

Despite the requirements for *RdgB2* for circadian photoentrainment and the PLR under scotopic conditions only, we found that *RdgB2*$^{-/-}$ mutant mice showed impairment in the b-wave but only under phototopic conditions. It is possible that RdgB2-positive amacrine cells contribute to the scotopic defects in circadian behavior by modulating synaptic input of rod bipolar cells to ipRGCs in the primary rod pathway (Figure 7). However, the scoto-

pic ERG data suggest that this subset of amacrine cells had little effect on rod bipolar cells. We suggest that RdgB2-positive amacrine cells are important in providing GABAergic inhibitory feedback to ON cone bipolar cells during light signaling (Figure 7). In addition, these results, along with the defects in the scotopic PLR of *RdgB2*$^{-/-}$ mice, suggest that rod input to ipRGCs most likely acts through the rod secondary pathway (Figure 7).

To account for the RdgB2 behavioral phenotypes under low-light conditions only, we propose a model in which expression of RdgB2 in GABA-positive amacrine cells contributes to the activity of ipRGCs under scotopic light conditions. Rod and cone bipolar cells express both GABA$_a$ and GABA$_c$ receptors at their axonal terminals and are modulated by inhibitory feedback from GABAergic amacrine cells (Lukasiewicz and Werblin, 1994; Pan and Lipton, 1995; Dong and Werblin, 1998; Euler and Wässle, 1998). This feedback is necessary to maintain sensitivity in the cone bipolar neurons. We suggest that RdgB2-positive amacrine cells provide inhibitory input to ON cone bipolar cells through GABA receptors (Figure 7), which helps to maintain bipolar cell sensitivity and modulate signaling into ipRGCs.

Concluding remarks
We conclude that loss of RdgB2 in a subset of GABAergic amacrine cells results in impairment in rod-driven signaling to ipRGCs. This in turn results in reduced PLR and circadian photoentrainment under dim light. In further support of the contribution of *RdgB2* to rod-driven input to the ipRGCs, the *RdgB2*$^{-/-}$ phenotype was no more severe after genetic ablation of rod photoreceptor cells. Our results indicate that the RdgB2 protein and RdgB2-expressing amacrine cells function at an important juncture connecting light signaling from image-forming rod photoreceptors to the non–image-forming ipRGCs.

MATERIALS AND METHODS
RdgB2$^{-/-}$ mice
Charles River Laboratories (Wilmington, MA) reconstituted the *RdgB2*$^{-/-}$ mice from embryos with permission from Tiansen Li (Lu *et al.*, 2001).

Consensual pupillary light reflex
We housed the animals individually in standard cages with food and water ad libitum and exposed the mice to 12 h:12 h light/dark cycles for at least 1 wk before testing. We performed all experiments using 8- to 16-wk-old mice of either sex and during the animals' day (ZT4-8). The mice were restrained by hand and not anesthetized. We dark-adapted the animals for ≥30 min before testing and then recorded movies of the pupillary constriction using an infrared light source and a Sony Handycam. We recorded ≥5 s from one eye in the dark to acquire the dark-adapted pupil size. Then we monitored pupillary constriction in that eye while delivering a ≥30-s light stimulus to the other eye using a 471-nm LED light (SuperBrightLEDs, St. Louis, MO) and a microscope light source with gooseneck arms to project the light directly on the eye. Before exposing the animals to additional light intensities using neutral density filters (Rosco Laboratories, Stamford, CT), we first dark-adapted the animals for
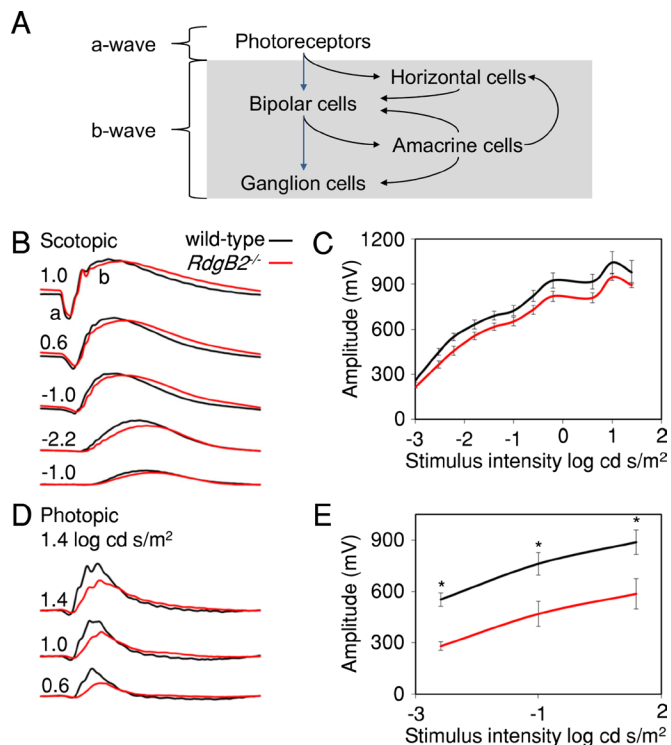
FIGURE 5: Electroretinogram recordings of light responses.
(A) Diagram of light transduction in the retina. The visual pathway begins with the activation of photoreceptors in the outer retina and generates the ERG a-wave. Activation of the cells in the gray box comprises the ERG b-wave. The arrows indicate the direction of signal transmission between cells. In the vertical pathway (indicated by the blue arrows), photoreceptor cells and bipolar cells release glutamate. Horizontal cells signal through the release of GABA. Amacrine cells are a diverse group of interneurons that can signal through the release of glycine, GABA, or dopamine. (B–E) Wild-type (black traces and lines) and $RdgB2^{-/-}$ mice (red traces and lines). (B) Scotopic ERG recordings from wild-type and $RdgB2^{-/-}$ mice. The light flash intensity is indicated on each trace (log cd m^{-2} s^{-1}); a-wave (a) and b-wave (b). (C) Scotopic b-wave amplitude. (D) Phototopic ERG recordings from wild-type and $RdgB2^{-/-}$ mice. (E) Photopic b-wave amplitude. ERG data were recorded from both eyes and averaged at each light intensity. Wild-type, $n = 4$; $RdgB2^{-/-}$, $n = 3$. Error bars indicate ±SEM. For statistical analysis, we used two-way unpaired Student's t tests. Asterisk indicates a significant difference ($p \leq 0.05$).

≥30 min. We measured light intensities using a calibrated spectrometer (Ocean Optics, Dunedin, FL), which allowed us to convert absorbance units to photons/cm^2 per second. The measured photon densities were then multiplied by the effective collecting area of a rod at the pupil (0.20 μm^2/rod), resulting in an estimate of the number of photoisomerizations per rod (R*/rod per second) (Lyubarsky and Pugh, 1996). This product was finally adjusted by fitting the values to a nomogram of rhodopsin with a $\lambda_{max} = 500$ nm to estimate the maximum number of R*/rod per second. We exported the movies to a computer, obtained movie stills using a VLC Media Player, and analyzed the pupil area using ImageJ software (National Institutes of Health, Bethesda, MD).

Immunohistochemistry on retinal slices

Mice of either sex were killed and enucleated at the ages of 8–16 wk. The eyes were fixed in 4% paraformaldehyde for 30 min at room temperature and washed three times with phosphate-buffered saline (PBS). We incubated all samples in 30% sucrose in PBS over-

night, embedded and froze the retinas in OCT medium, and cut 20-μm sections, which we fixed to microscope slides. For staining, we blocked and permeabilized the sections with blocking buffer (5% normal goat serum and 0.3% Triton X-100 in PBS) for 1 h at room temperature. We incubated the sections with the following primary antibodies in blocking buffer for 48 h at 4°C: 1) rabbit anti-RdgB2, 1:200 dilution, 2) mouse anti-PKCα, 1:1000 dilution (Invitrogen, Grand Island, NY), 3) guinea pig anti-GABA, 1:1500 dilution (Abcam, Cambridge, MA), 4) chicken anti–β-galactosidase (Abcam), and 5) chicken anti–tyrosine hydroxylase, 1:1000 dilution. The sections were next washed five times with PBS and then incubated for 1 h at room temperature with the following secondary antibodies in blocking buffer: 1) Alexa Fluor 647 anti-rabbit, 2) Alexa Fluor 488 anti-mouse, 3) Alexa Fluor 488 anti-guinea pig, and 4) Alexa Fluor 488 anti-chicken. The slides were washed five times with PBS and mounted in VECTASHIELD Mounting Media.

Multielectrode array recordings

We used $RdgB2^{-/-}$ mice and their wild-type littermates of either sex between the ages of 5 and 6 mo. We dark-adapted the animals overnight and performed all surgical procedures under dim red light. We killed the mice with CO_2, dissected the retinas, removed all pigmented epithelium, and placed the photoreceptor side down onto a filter membrane (Anodisc; Whatman, Piscataway, NJ). We then transferred the membrane onto a 60-channel multielectrode array (60MEA200/30iR-ITO-gr; Multi Channel System MCS, Reutlingen, Germany) with the RGC layer facing the array. Retinas were superfused continuously at 3–4 ml/min with oxygenated bicarbonate-buffered Ames' medium (Sigma, St. Louis, MO) and maintained at 32°C with a temperature controller (TC-324B; Warner Instruments, Hamden, CT). To stabilize the spike amplitudes, we superfused the retinas with media for 1 h before beginning the recordings. We blocked signaling from rod and cone photoreceptors to the inner retina by application of a pharmacological cocktail containing 50 μM L-(+)-2-amino-4-phosphonobutyric acid (Tocris, Ellisville, MO), 40 μM 6,7-dinitroquinoxaline-2,3-dione (Tocris), and 30 μM D-(-)-2-amino-5-phosphonopentanoic acid (Tocris).

We kept the retinas in complete darkness except when irradiating with the test stimuli. We identified ipRGCs on the basis of their characteristic sluggish, persistent light responses, which they exhibited in the presence of the pharmacological cocktail. We generated 10-s full-field white-light stimuli using a tungsten-halogen microscopy illuminator (model EW-09741-50; Cole-Parmer Instruments, Vernon Hills, IL) equipped with a custom-made electromechanical shutter. We delivered the light onto the retinas with a fiber optic cable. We adjusted stimulus intensities by introducing neutral density filters (Newport Oriel Instruments, Stratford, CT) into the light path. The unattenuated (0 log) intensity (480 nm) at the surface of the preparation was 6.0×10^{12} photons/cm^2 per second.

Amplified voltage data were digitized at 10 kHz using a PC-based A/D interface card and MC Rack software (MCS). We set the spike detection threshold for each channel at three to four times the SD of the voltage, and we bandpass filtered the signals (200 to 3 kHz) and stored them. We performed cluster analysis of the spike data using Offline Sorter software (Plexon, Dallas, TX). We further analyzed the spike trains with OriginPro 8.0 (OriginLab, Northampton, MA) and Excel 2007 (Microsoft, Redmond, WA) to quantify 1) the peak firing rate, which we calculated by subtracting the spontaneous resting firing rate during the 10 s preceding the light stimulation from the maximal firing rate during the light stimulus, 2) total spikes, which we calculated by subtracting the number of spikes during the 10 s preceding light onset from the sum of all action potentials occurring
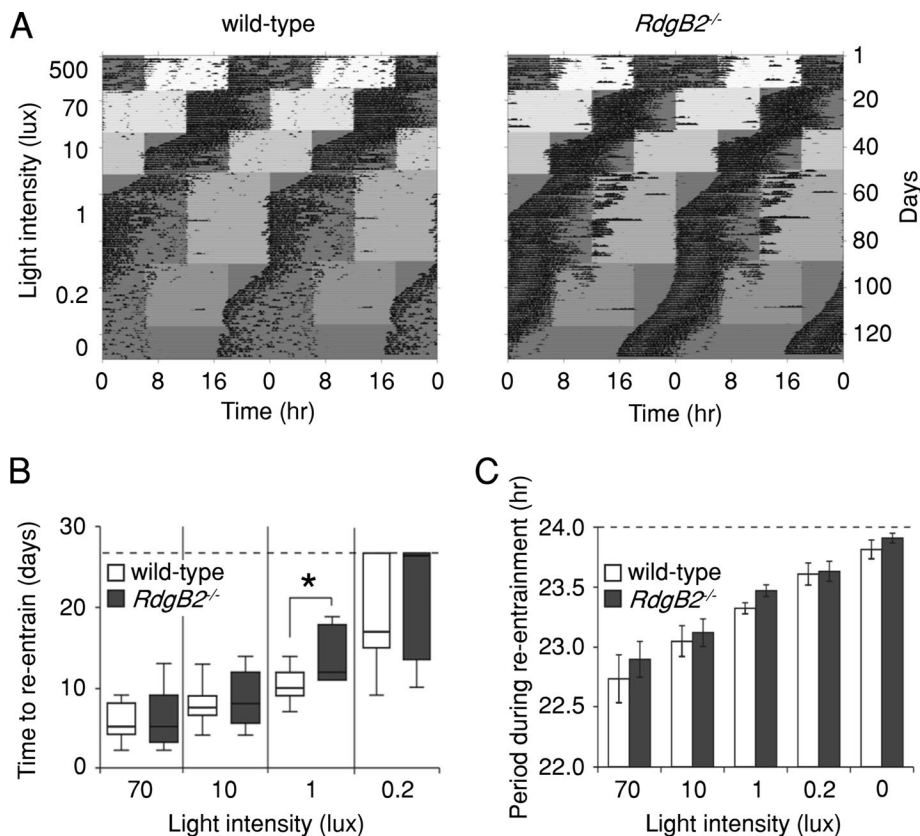
FIGURE 6: Circadian photoentrainment assays. (A) Representative double-plotted wheel-running actograms for wild-type and RdgB2−/− mice with decreasing light intensities during the light period. The 12-h dark periods are denoted by a dark gray background. (B) Plot of the group distribution and median number of days to reentrain to a 6-h shift in the light period with decreasing steps in light intensity. The bars define the distribution for the entire group. The boxes show activity of 50% of the group between the 25th and 75th percentile, and the lines indicate the median for the group. For the statistical analysis, we used the two-tailed Mann–Whitney U test. *$p \leq 0.05$. (C) Length of the running periods for the mice during photoentrainment at decreasing steps in light intensity. Wild-type, $n = 8$; RdgB2−/−, $n = 10$.
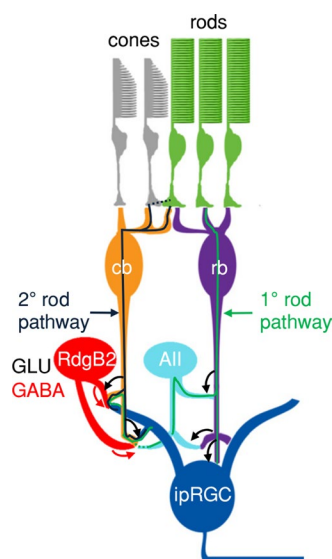
during the light stimulus, 3) peak latency, which we calculated as the time gap between stimulus onset and the time of peak firing rate, and 4) half decay time, calculated as the time gap between the time of peak firing rate and the time when the firing frequency deceased to the half of the peak.

ERG recordings

We dark-adapted 6- to 8-wk-old mice of either sex overnight and performed all procedures under dim red light. We anesthetized the mice by intraperitoneal injection of a ketamine hydrochloride/xylazine (100 and 5 mg/kg, respectively) mixture. To perform the recordings, we kept the mice on a 39°C heating pad and dilated their eyes with Midrin P (0.5% tropicamide and 0.5% phenylephrine hydrochloride; Santen Pharmaceutical, Osaka, Japan). We inserted a subdermal ground electrode into the tail and placed the reference electrode under the skin between the ears and caudal to the eyes. We lubricated the cornea of each eye with gonioscopic prism solution (Alcon Labs, Fort Worth, TX) and then set platinum loop recording electrodes on the coated surface of each eye. We delivered the light stimulation to both eyes with a Ganzfeld bowl illuminator. We first tested the mice under scotopic light intensities, using 11 increasing light steps ranging from −3.00 to 1.40 log cd m^{-2} s^{-1}. After the scotopic test, we irradiated both eyes with an ambient light of 1.00 log cd m^{-2} s^{-1} for 10 min in preparation for the photopic recordings. During the photopic test, we exposed the mice to three increasing light steps (0.60, 1.00, and 1.40 log cd m^{-2} s^{-1}) on top of the ambient light.

Circadian wheel-running behavior

We housed animals individually in wheel-running cages (wheel attached to the lid of the cage) under 12 h:12 h light/dark cycles and tested animals of either sex between the ages of 8 and 16 wk. The cages were then housed in a larger, temperature-controlled black box that held multiple cages. Every few weeks, the light cycles were advanced 6 h and the light intensities were decreased using neutral density filters (Rosco). Light intensities at the surfaces of the cages were measured using a luminometer (EXTECH, Burlington, VT). To determine the number of days needed for photoentrainment, we defined photoentrainment as the day when the circadian period stabilized to ~24 h and the onset of activity was near the onset of darkness. We monitored the revolutions using VitalView software (MiniMitter, Oakmont, PA) and visualized and analyzed the data using Clocklab (Actimetrics, Wilmette, IL).

FIGURE 7: Diagram of rod-driven light input into ipRGCs. The primary (1°) rod pathway is indicated by the green line, and the secondary (2°) rod pathway is indicated by the blue line. The dotted line indicates a gap junction. Glutamate (GLU) release from bipolar cells is indicated by the black arrows, and GABA release from the RdgB2-positive amacrine cells is indicated by the red arrows. ipRGC is a representation of all melanopsin-expressing ganglion cells. Cone bipolar cells (cb), rod bipolar cells (rb), AII amacrine cells (AII), RdgB2-expressing amacrine cell (RdgB2).

Statistical analyses

We used unpaired Student's t tests and one-way analysis of variance and Tukey post hoc test to determine statistical significance of pupillary constriction data. For MEA recordings and ERG data, we used unpaired Student's t tests to determine statistical significance. We analyzed the statistical significance of the circadian wheel-running data using the Mann–Whitney U test. In all tests, $p \leq 0.05$ is considered significant and indicated by an asterisk.

REFERENCES

Altimus CM, Güler AD, Alam NM, Arman AC, Prusky GT, Sampath AP, Hattar S (2010). Rod photoreceptors drive circadian photoentrainment across a wide range of light intensities. Nat Neurosci 13, 1107–1112.

Altimus CM, Güler AD, Villa KL, McNeill DS, Legates TA, Hattar S (2008). Rods-cones and melanopsin detect light and dark to modulate sleep independent of image formation. Proc Natl Acad Sci USA 105, 19998–20003.

Asari H, Meister M (2012). Divergence of visual channels in the inner retina. Nat Neurosci 15, 1581–1589.

Berson DM (2007). Phototransduction in ganglion-cell photoreceptors. Pflugers Arch 454, 849–855.

Berson DM, Dunn FA, Takao M (2002). Phototransduction by retinal ganglion cells that set the circadian clock. Science 295, 1070–1073.

Chávez AE, Grimes WN, Diamond JS (2010). Mechanisms underlying lateral GABAergic feedback onto rod bipolar cells in rat retina. J Neurosci 30, 2330–2339.

Chávez AE, Singer JH, Diamond JS (2006). Fast neurotransmitter release triggered by Ca influx through AMPA-type glutamate receptors. Nature 443, 705–708.

Demb JB, Singer JH (2012). Intrinsic properties and functional circuitry of the AII amacrine cell. Vis Neurosci 29, 51–60.

Dong CJ, Werblin FS (1998). Temporal contrast enhancement via GABA$_C$ feedback at bipolar terminals in the tiger salamander retina. J Neurophysiol 79, 2171–2180.

Dumitrescu ON, Pucci FG, Wong KY, Berson DM (2009). Ectopic retinal ON bipolar cell synapses in the OFF inner plexiform layer: contacts with dopaminergic amacrine cells and melanopsin ganglion cells. J Comp Neurol 517, 226–244.

Eggers ED, Lukasiewicz PD (2006). GABA$_A$, GABA$_C$ and glycine receptor-mediated inhibition differentially affects light-evoked signalling from mouse retinal rod bipolar cells. J Physiol 572, 215–225.

Euler T, Wässle H (1998). Different contributions of GABA$_A$ and GABA$_C$ receptors to rod and cone bipolar cells in a rat retinal slice preparation. J Neurophysiol 79, 1384–1395.

Freedman MS, Lucas RJ, Soni B, von Schantz M, Munoz M, David-Gray Z, Foster R (1999). Regulation of mammalian circadian behavior by non-rod, non-cone, ocular photoreceptors. Science 284, 502–504.

Gooley JJ, Lu J, Fischer D, Saper CB (2003). A broad role for melanopsin in nonvisual photoreception. J Neurosci 23, 7093–7106.

Güler AD, Ecker JL, Lall GS, Haq S, Altimus CM, Liao HW, Barnard AR, Cahill H, Badea TC, Zhao H, et al. (2008). Melanopsin cells are the principal conduits for rod-cone input to non-image-forming vision. Nature 453, 102–105.

Harris WA, Stark WS (1977). Heriditary retinal degeneration in *Drosophila melanogaster*: a mutant defect associated with the phototransduction process. J Gen Physiol 69, 261–291.

Hattar S, Kumar M, Park A, Tong P, Tung J, Yau KW, Berson DM (2006). Central projections of melanopsin-expressing retinal ganglion cells in the mouse. J Comp Neurol 497, 326–349.

Hattar S, Liao HW, Takao M, Berson DM, Yau KW (2002). Melanopsin-containing retinal ganglion cells: architecture, projections, and intrinsic photosensitivity. Science 295, 1065–1070.

Hattar S, Lucas RJ, Mrosovsky N, Thompson S, Douglas RH, Hankins MW, Lem J, Biel M, Hofmann F, Foster RG, Yau KW (2003). Melanopsin and rod-cone photoreceptive systems account for all major accessory visual functions in mice. Nature 424, 76–81.

Isoldi MC, Rollag MD, Castrucci AM, Provencio I (2005). Rhabdomeric photototransduction initiated by the vertebrate photopigment melanopsin. Proc Natl Acad Sci USA 102, 1217–1221.

Kolb H (1995). Roles of amacrine cells. In: Webvision: The Organization of the Retina and Visual System [Internet], ed. H Kolb, E Fernandez, and R Nelson, Salt Lake City: University of Utah Health Sciences Center. Retrieved 20 June 2013 from www.ncbi.nlm.nih.gov/books/NBK11539/.

Kolb H (1997). Amacrine cells of the mammalian retina: neurocircuitry and functional roles. Eye (Lond) 11, 904–923.

Lu C, Peng YW, Shang J, Pawlyk BS, Yu F, Li T (2001). The mammalian *retinal degeneration B2* gene is not required for photoreceptor function and survival. Neuroscience 107, 35–41.

Lu C, Vihtelic TS, Hyde DR, Li T (1999). A neuronal-specific mammalian homolog of the *Drosophila* retinal degeneration B gene with expression restricted to the retina and dentate gyrus. J Neurosci 19, 7317–7325.

Lucas RJ, Hattar S, Takao M, Berson DM, Foster RG, Yau KW (2003). Diminished pupillary light reflex at high irradiances in melanopsin-knockout mice. Science 299, 245–247.

Lukasiewicz PD, Werblin FS (1994). A novel GABA receptor modulates synaptic transmission from bipolar to ganglion and amacrine cells in the tiger salamander retina. J Neurosci 14, 1213–1223.

Lyubarsky AL, Pugh EN Jr (1996). Recovery phase of the murine rod photoresponse reconstructed from electroretinographic recordings. J Neurosci 16, 563–571.

Masland RH (2011). Cell populations of the retina: the Proctor lecture. Invest Ophthalmol Vis Sci 52, 4581–4591.

Milligan SC, Alb JG Jr, Elagina RB, Bankaitis VA, Hyde DR (1997). The phosphatidylinositol transfer protein domain of *Drosophila* retinal degeneration B protein is essential for photoreceptor cell survival and recovery from light stimulation. J Cell Biol 139, 351–363.

Mrosovsky N, Hattar S (2003). Impaired masking responses to light in melanopsin-knockout mice. Chronobiol Int 20, 989–999.

Nickle B, Robinson PR (2007). The opsins of the vertebrate retina: insights from structural, biochemical, and evolutionary studies. Cell Mol Life Sci 64, 2917–2932.

Østergaard J, Hannibal J, Fahrenkrug J (2007). Synaptic contact between melanopsin-containing retinal ganglion cells and rod bipolar cells. Invest Ophthalmol Vis Sci 48, 3812–3820.

Pan ZH, Lipton SA (1995). Multiple GABA receptor subtypes mediate inhibition of calcium influx at rat retinal bipolar cell terminals. J Neurosci 15, 2668–2679.

Perez De Sevilla Müller L, Shelley J, Weiler R (2007). Displaced amacrine cells of the mouse retina. J Comp Neurol 505, 177–189.

Qiu X, Kumbalasiri T, Carlson SM, Wong KY, Krishna V, Provencio I, Berson DM (2005). Induction of photosensitivity by heterologous expression of melanopsin. Nature 433, 745–749.

Schmidt M, Wässle H, Humphrey M (1985). Number and distribution of putative cholinergic neurons in the cat retina. Neurosci Lett 59, 235–240.

Schubert T, Hoon M, Euler T, Lukasiewicz PD, Wong RO (2013). Developmental regulation and activity-dependent maintenance of GABAergic presynaptic inhibition onto rod bipolar cell axonal terminals. Neuron 78, 124–137.

Smith BJ, Tremblay F, Côté PD (2013). Voltage-gated sodium channels contribute to the b-wave of the rodent electroretinogram by mediating input to rod bipolar cell GABA$_C$ receptors. Exp Eye Res 116, 279–290.

Terakita A (2005). The opsins. Genome Biol 6, 213.

Van Hook MJ, Wong KY, Berson DM (2012). Dopaminergic modulation of ganglion-cell photoreceptors in rat. Eur J Neurosci 35, 507–518.

Weng S, Estevez ME, Berson DM (2013). Mouse ganglion-cell photoreceptors are driven by the most sensitive rod pathway and by both types of cones. PLoS One 8, e66480.

Wong KY, Dunn FA, Berson DM (2005). Photoreceptor adaptation in intrinsically photosensitive retinal ganglion cells. Neuron 48, 1001–1010.

Wong KY, Dunn FA, Graham DM, Berson DM (2007). Synaptic influences on rat ganglion-cell photoreceptors. J Physiol 582, 279–296.

Xue T, Do MT, Riccio A, Jiang Z, Hsieh J, Wang HC, Merbs SL, Welsbie DS, Yoshioka T, Weissgerber P, et al. (2011). Melanopsin signalling in mammalian iris and retina. Nature 479, 67–73.

Zhang C, McCall MA (2012). Receptor targets of amacrine cells. Vis Neurosci 29, 11–29.